MODEL INDEPENDENT CONSTRAINTS ON THE IONIZATION HISTORY

JOHN ZANAZZI, NORTHERN ARIZONA UNIVERSITY

1. ABSTRACT

We present a model independent eigenmode analysis of the ionization history around recombination and before reionization. This analysis uses only data which could be gathered from a power spectrum analysis of the cosmic microwave background, and simulates changes in the fiducial model of the ionization history. A perturbative method is used to obtain numerical derivatives $\frac{\partial C_l}{\partial X_i}$, where X_i are perturbations of the ionization history at various redshift values. The marginalized Fisher matrix obtained from this set of derivatives is then diagonalized to obtain the model independent principal components for the ionization history.

2. INTRODUCTION

The subject for this summer project was a quantitiy known to cosmologists called the free electron fraction X_e. The free electron fraction is defined as

$$X_e \equiv \frac{n_e}{n_H - n_e}$$

where n_e denotes the number density of free electrons and n_H denotes the number density of Hydrogen atoms. This value states empirically how ionized the universe is: when $X_e = 0$, the universe is completely un-ionized, and when $X_e = 1$, the universe is completely ionized.

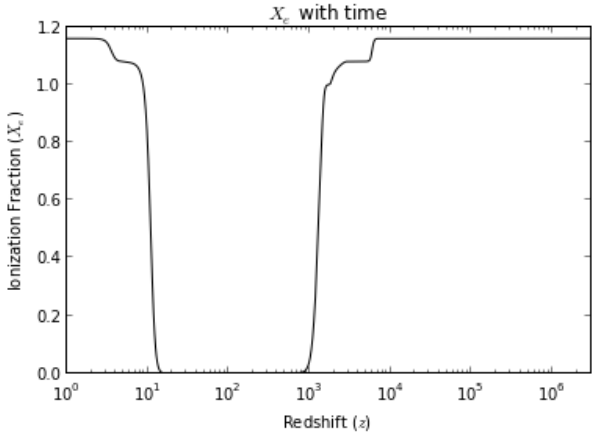

FIGURE 1. The Free Electron Fraction X_e as a function of Redshift z.

Shown on figure 1 is the Ionization history. Here, redshift z is defined as

$$1+z \equiv \frac{\lambda_{\text{obs}}}{\lambda_{\text{emit}}} = \frac{1}{a}$$

where a is the scale factor, and λ are the wavelengths of emitted and observed light. The period around $z \sim 10$ is typically called reionization, $z \sim 10$ to 800 typically is called the ionization floor, $z \sim 800$ to 1200 is called recombination, and $z \sim 1200$ on is typically called the ionization ceiling. There are a number of reasons why this quantity is worth studying.

The first is that the Planck Collaboration will soon release the results of an all sky survey which places further constraints on the Cosmic Microwave Background (CMB) power spectrum. This increased accuracy will be in the multipole moment range of $\ell = 200$ to 2000. Because the Planck data will constrain our cosmological parameters further, this motivates an in depth study on the constraints for these values. The quantity which will be studied in this analysis is the ionization history (quantified by the free electron fraction X_e) and how well constrained the values of X_e are for various redshifts z around recombination.

In addition, competing models of dark matter predict how strong the electromagnetic interactions between constituting particles are during the beginning of the universe. This in turn alters the values of the free electron fraction X_e at a number of redshift values z. By studying X_e, data which supports or rejects various models may be gathered.

Furthermore, the ionization history is a fundamental quantity of our universe purely in the realm of atomic physics. By studying how strongly X_e is constrained by power spectrum data, we can see how much of the ionization history is determined purely by the CMB power spectrum.

3. METHODS

We begin with the defnition for the Power Spectrum. Let Θ^X be the perturbation in a given distribution. In this analysis, $X = T, E$, representing photon temperature and polarization perturbations. This perturbation may be expanded in terms of the spherical harmonics Y_{lm}:

$$\Theta^X(\vec{x}, \hat{p}, \eta) = \sum_{l=1}^{\infty} \sum_{m=-l}^{l} a^X_{lm}(\vec{x}, \eta) Y_{lm}(\hat{p})$$

where $\vec{x}$ denotes position, $\hat{p}$ denotes direction, and η represents the conformal time. From this, we may define the power spectrum C_l^{XY} as

$$\langle a^X_{lm}, a^{Y*}_{l'm'} \rangle = \delta_{ll'}\, \delta_{mm'}\, C_l^{XY}$$

where δ_{ij} denotes the Kronecker delta function. From this, we may define the Fisher matrix in [5] as

$$F_{ij} = \sum_l \sum_{X,Y} \frac{\partial C_l^X}{\partial s_i} \text{Cov}^{-1}(\hat{C}_l^X, \hat{C}_l^Y) \frac{\partial C_l^Y}{\partial s_j}$$

Here s_i are any cosmological parameters and X, Y vary between TT, EE, and TE corresponding to temperature and polarization components of the power spectrum C_l. The diagonal components of the covariance matrix are

$$\text{Cov}((\hat{C}_l^{TT})^2) = \frac{2}{(2l+1) f_{\text{sky}}} (C_l^{TT} + N_l^T)^2$$

$$\text{Cov}((\hat{C}_l^{EE})^2) = \frac{2}{(2l+1) f_{\text{sky}}} (C_l^{EE} + N_l^E)^2$$

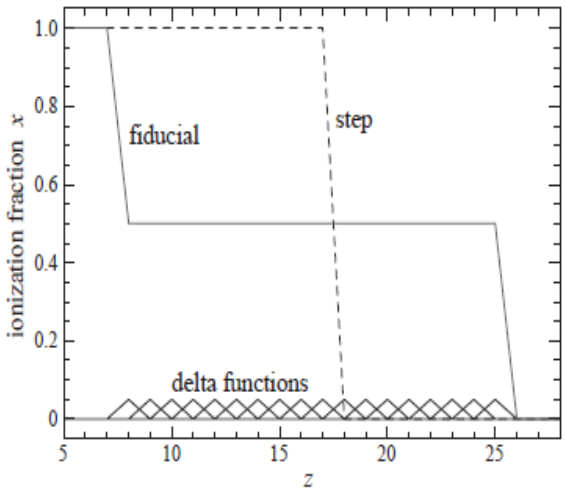

FIGURE 2. Delta Functions

$$\mathrm{Cov}((\hat{C}_l^{TE})^2) = \frac{1}{(2l+1)f_{\mathrm{sky}}}((C_l^{TE})^2 + (C_l^{TT}+N_l^T)(C_l^{EE}+N_l^E))$$

and the off diagonal components of the covariance matrix are

$$\mathrm{Cov}(\hat{C}_l^{TT}\hat{C}_l^{EE}) = \frac{2}{(2l+1)f_{\mathrm{sky}}}(C_l^{TE})^2$$

$$\mathrm{Cov}(\hat{C}_l^{TT}\hat{C}_l^{TE}) = \frac{2}{(2l+1)f_{\mathrm{sky}}}C_l^{TE}(C_l^{TT}+N_l^T)$$

$$\mathrm{Cov}(\hat{C}_l^{EE}\hat{C}_l^{TE}) = \frac{2}{(2l+1)f_{\mathrm{sky}}}C_l^{TE}(C_l^{EE}+N_l^E)$$

where f_{sky} is the fraction of sky covered in the survey, and N_l is the total noise at multipole moment l from the T and E measurements respectively. The N_l values were obtained from [1] and [3]. The Fisher matrix is a way to parameterize how well determined a set of parameters are with respect to a given power spectrum. Because we wanted to learn how well determined sections of the free electron fraction were, what we need is a set of perturbation functions δX_i of X_e. Once this set of perturbation functions is defined, we may take derivatives $\frac{\partial C_l}{\partial X_i}$ to determine how well constrained sections of X_e are. In [2], X_e around reionization ($z = 8-25$) was analyzed by a set of "delta functions," displayed in figure 2. Note that a "delta function" is a single triangle perturbed at some z value, not a sequence of triangle waves.

This project began by applying the method used in [2] to a different section of X_e: namely, $z = 50$ to 2000 which consists of the ionization floor, recombination, and a bit of the ionization ceiling. However, the Fortran code CAMB had numerical problems with the width, height, and lack of smoothness of the Delta functions, so a new method of parameterizing X_e was needed to obtain well behaved derivatives. What was done was perturb X_e by a sum of delta functions, to create a set of "table functions," displayed in figure 3.

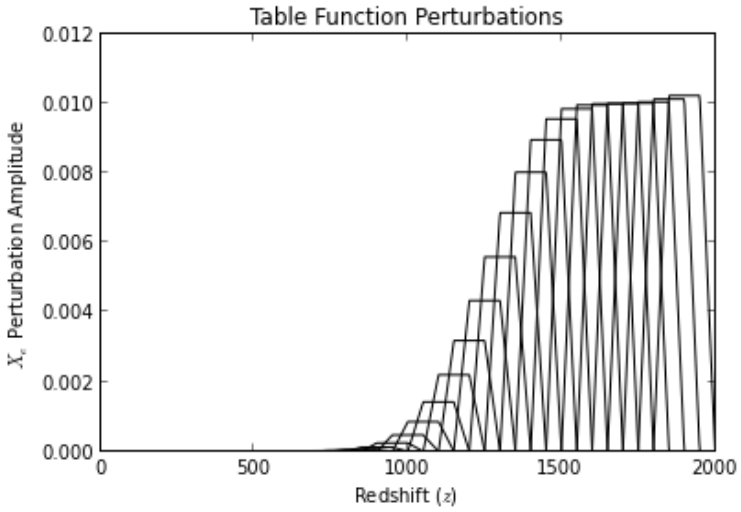

FIGURE 3. Table Funtions

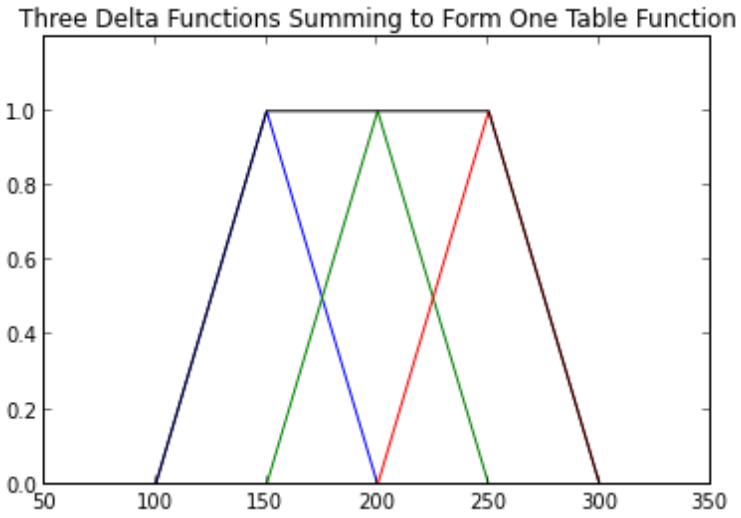

FIGURE 4. Delta Functions Summing to a Table Function

These table functions may be thought of as a linear sum of a number of delta functions, so the method is simply an extension of [2]. A visualization of one such some is shown in figure 4. The advantages of perturbing X_e by table functions instead of delta functions were numerous:

1. Because the table functions overlapped, when the table functions were summed to create the eigenmodes, one delta function was in a sense averaged by the amplitudes of the

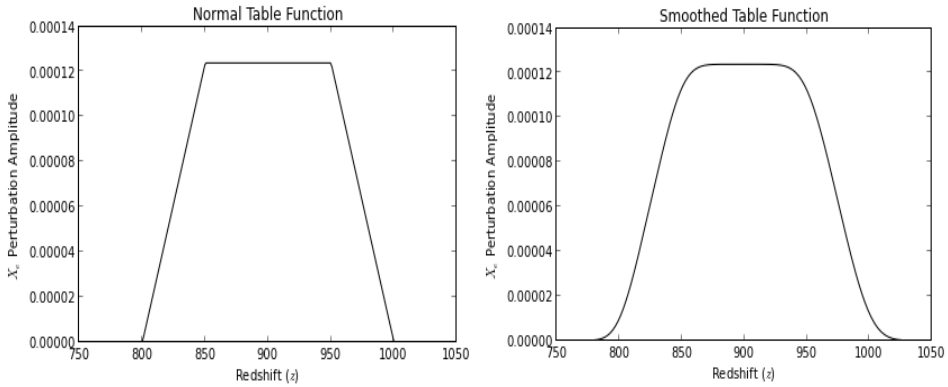

FIGURE 5. Table Smoothing

surrounding table functions. However, these averages were physical as opposed to a numerical smoothing algorithm applied to the resultant Fisher matrix.

2. The table functions behaved well numerically due to their width, but because they could be created by delta functions of any width, the table functions could be placed close to one another. This made it possible to perturb X_e more finely while still obtaining reasonable numerical behavior, as opposed to wide delta functions which had to be placed far apart from one another.

3. Linear combinations of table functions still obtained structures which behaved well numerically. Delta functions did this as well, but other closely space perturbation functions thought of by the author lacked this advantage.

The height of the table functions was determined by the center of the function, and set by multiplying the value of X_e at the center of the table function by a constant value of $dY = 0.01$. In addition, a smoothing algorithm was applied to individual table functions so that the numerical behavior was more well behaved. The basic structure was left intact, so all that was done was "smooth the edges" of the table functions, shown in figure 5.

To take the derivatives $\frac{\partial C_l}{\partial X_i}$, a linear approximation was made to obtain the values numerically. First, the fiducial X_e was perturbed by a given table function δX_i. This perturbed free electron fraction $X_e + \delta X_i$ was then fed into CAMB to calculate the C_l's of the perturbed model power spectrum. An output power spectrum $C_l + \Delta C_l$ was then obtained. To approximate $\frac{\partial C_l}{\partial X_i}$, the following expression was calculated:

$$\frac{\partial C_l}{\partial X_i} \approx \frac{(C_l + \Delta C_l) - C_l}{\Delta X_i} = \frac{\Delta C_l}{\Delta X_i}$$

Where ΔX_i is the amplitude height of the delta function δX_i. These numerical approximations for the derivatives $\frac{\partial C_l}{\partial X_i}$ were then marginalized over the standard cosmological parameters. In other words, a new Fisher matrix $\mathscr{F}$ was calculated that included derivatives of C_l with respect to the standard cosmological parameters. We let the components s_i range between $\delta X_i, A_s, n_s, \Omega_b h^2, \Omega_c h^2, \tau$, and H_0. Finally, to calculate the marginalized Fisher matrix F_{marg}, if $0 \leq i \leq k$ denotes the values of α_i which are δX_i, the following

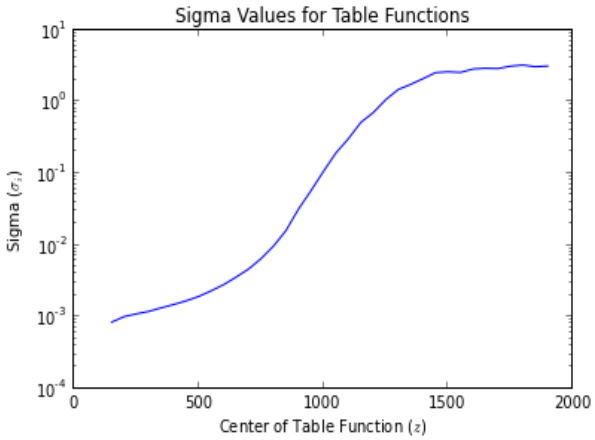

FIGURE 6. Sigma Values for Table Functions

matrix was calculated

$$G = \mathscr{F}^{-1}$$

$$F_{\text{marg}} = (G_{ij})^{-1}$$

where $0 \leq i, j \leq k$. The purpose of marginalizing $\mathscr{F}$ is to "taint" the delta functions with the influence from the standard cosmological parameters (This becomes useful when one runs Monte Carlo Markov Chains). Once F_{marg} was calculated, it was diagonalized to obtain the matrix R:

$$F_{\text{marg}} = R\,{\sigma_i}^{-2}\,R^{-1}$$

This matrix R was used to find the Principal Components of X_e, a set of orthogonal functions created by the perturbation functions δX_i and eigenmodes m_j, defined as

$$m_j \equiv R_{ij}\,\delta X_i$$

The way that m_j is defined makes it so that the most well determined functions m_j are those with the smallest values, as

$$\langle m_i, m_j \rangle = \delta_{ij}\,\sigma_i^2$$

where δ_{ij} is the Kronecker delta function, not to be confused with the perturbation functions δX_i. Thus we have obtained a set of model independent functions m_i which represent linear combinations of perturbation functions δX_i.

4. RESULTS

The sigma values obtained for the perturbation functions $\frac{\partial C_l}{\partial X_i}$ are presented in figure 6. Notice that the ionization floor ($z = 50 - 800$) is more well determined than the ionization ceiling ($z = 1200 - 2000$). This is to be expected, as the visibility function peaks at $z \sim 1100$. This means that anything before $z \sim 1100$ should have little effect on current observations, or any changes to X_e should not yet be visible. It should be noted that in order to calculate the Fisher matrix F given this set of derivatives, $\ell < 300$ was ignored due to the fact that the C_l's became slightly chaotic.

Next we examine the sigma values for the eigenmodes m_i in figure 7. We see that there are something on the order of ~ 25 eigenmodes which have signal to noise ratios less than

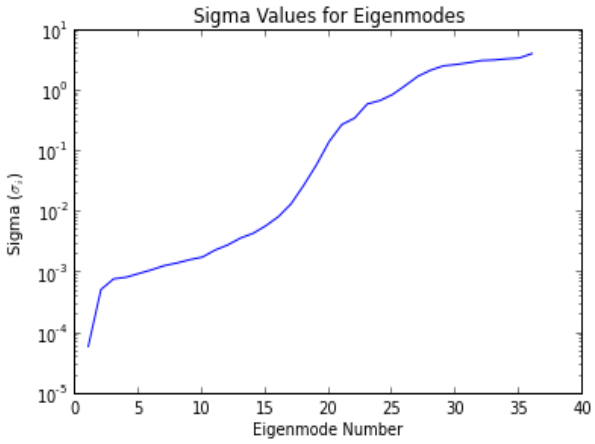

FIGURE 7. Eigenmode Sigma Values

one. The reason why there would be so many eigenmodes with useful information may be seen by looking at the plots for the eigenmodes themselves. The eigenmodes are indexed such that the best determined modes have the lowest indexes, and the least determined modes have the highest indexes. The eigenmodes themselves are presented in figure 8

Many eigenmodes perturb the ionization floor and recombination ($z = 50 - 1200$) portions of X_e, causing significant effects with respect to C_l. Also notice all the eigenmodes which have signal to noise ratios greater than one ($j = 25 - 35$) perturb mainly the ionization ceiling ($z = 1200 - 2000$).

For completeness, the table function amplitudes are included in figure 9. Notice the fact that the amplitudes are more noisy than the eigenmodes. This smoothing comes from the fact that the table functions overlap with one another, which allows the functions to be much smoother than their delta function counterparts.

Due to lack of time, the author of this paper was not able to compare these eigenmodes to competing theories for dark matter. However, it is noted that some theories predict a shift in the values of the ionization floor, which is the best determined section for the ionization history X_e, which may easily be seen by examining the first eigenmode. Reference [4] examined the case where just the ionization floor was perturbed.

5. CONCLUSIONS

We may deduce a number of facts which will be useful for further analysis of X_e. First, we see that the most constrained portion of X_e by far is the ionization floor. This is shown by examining the first eigenmode, which is the best determined eigenmode by a factor of 10, and is completely restricted to the ionization floor. In addition, we also see that the recombination history of X_e is also well constrained, as many of the most well constrained eigenmodes perturb the region $z = 800 - 1200$, in particular the third eigenmode.

Second, it is clear that the ionization ceiling is poorly determined by cosmological data. This may be seen by a combination of the fact that the covariance values are the highest for perturbation functions which have centers in the range of $z = 1200 - 2000$, and all eigenmodes which have signal to noise ratios greater than one perturb the ionization ceiling. Thus the region of X_e where $z > 1200$ is poorly determined by observational data.

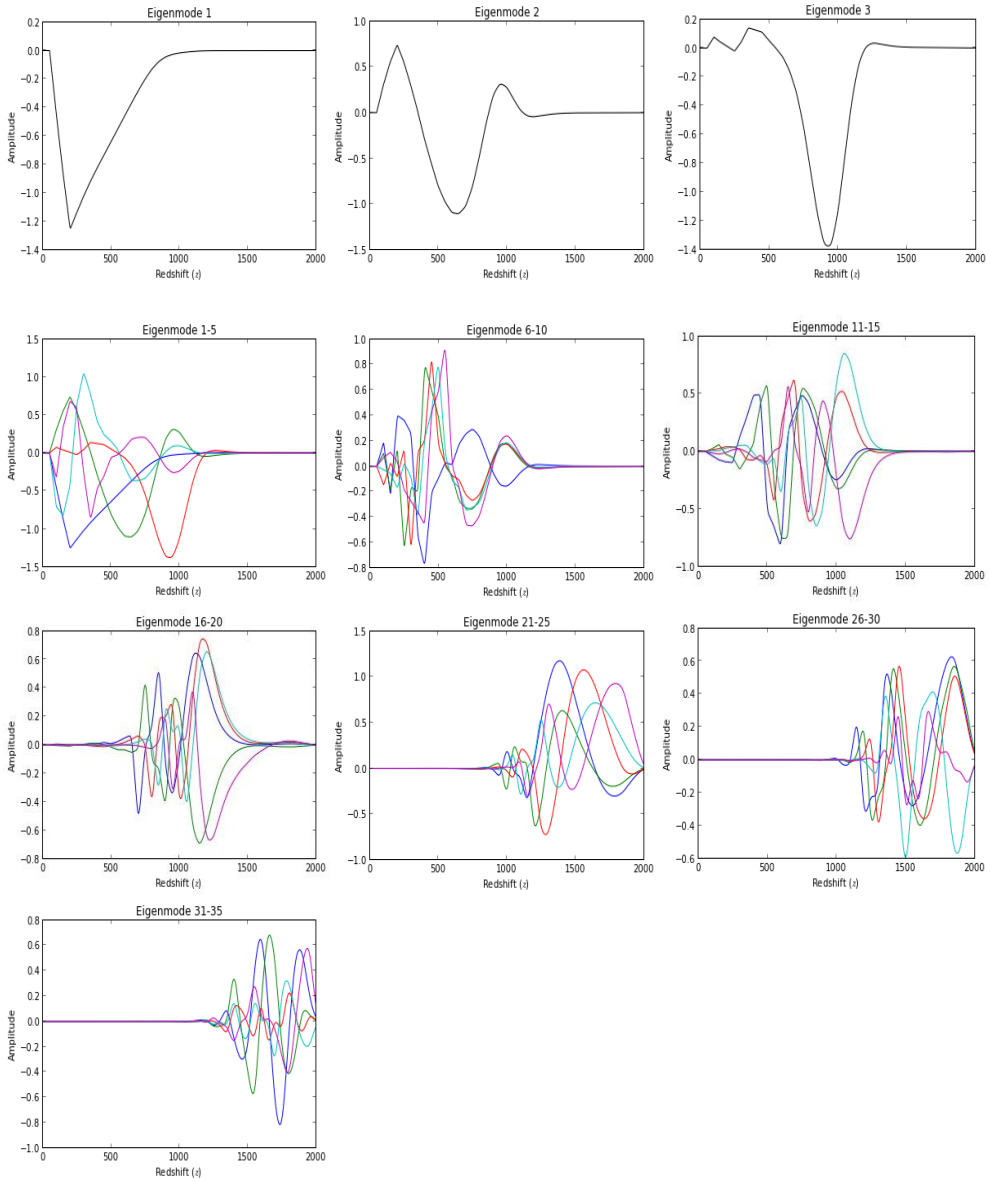

FIGURE 8. Eigenmodes. Best three determined eigenmodes are listed at the top.

One of the largest difficulties for this project was the fact that CAMB does not sample frequently around recombination. If CAMB where fixed such that this period of the Ionization History had more data points to perturb, eigenmodes which are less contaminated by noise would be able to be obtained.

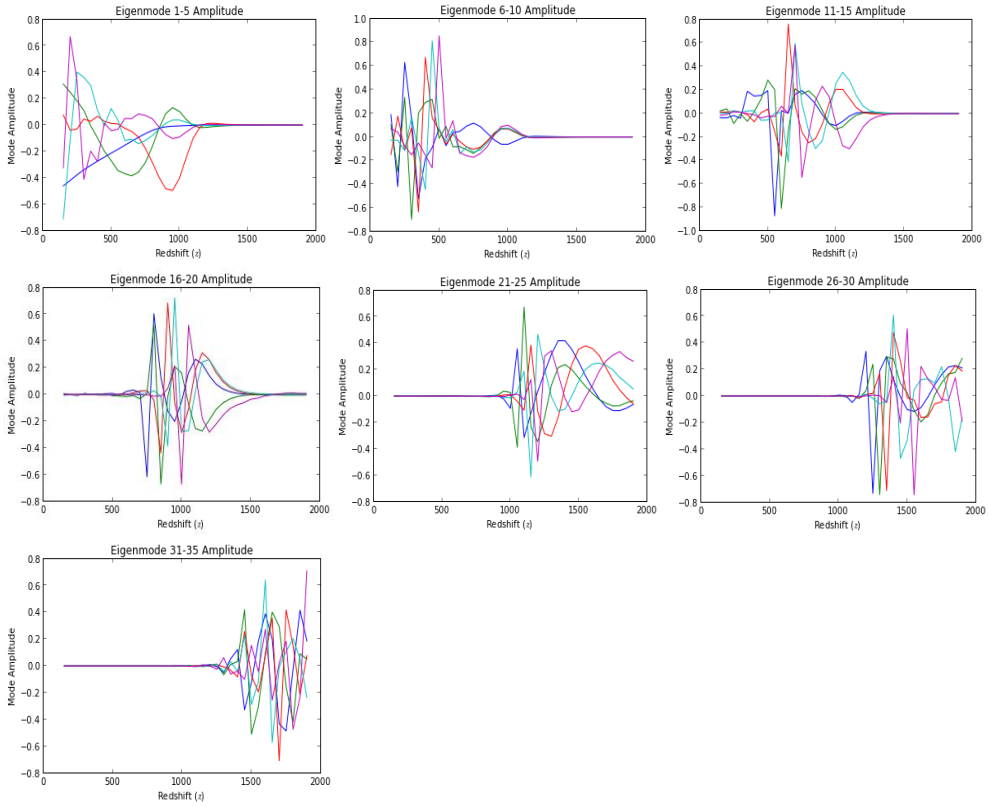

FIGURE 9. Eigenmode Amplitudes for Table functions. X-axis is Redshift (z) and y-axis is Table Function amplitude.

6. ACKNOWLEDGEMENTS

I would like to begin by thank all those in the Cosmology Group which I worked with, which consisted of Pr. Lloyd Knox, Marius Millea, and Bent Follin. These individuals helped me understand the fundamentals of the subject which I was working on, debug code, and were a sound board to new ideas. Next I would like to thank Pr. Rena Zieve, director of the Physics Research Experiences for Undergraduates Program at the University of California Davis, for organizing the REU program and REU related events. Last, I would like to thank the National Science Foundation for funding this research.

REFERENCES

[1] R. Keisler et. al. A measurement of the damping tail of the cosmic microwave background power spectrum with the south pole telescope. *The Astrophysical Journal*, 743(1):28, 2011.

[2] Wayne Hu and Gilbert P. Holder. Model-independent reionization observables in the cmb. *Phys. Rev. D*, 68:023001, Jul 2003.

[3] N. Jarosik, C. L. Bennett, J. Dunkley, B. Gold, M. R. Greason, M. Halpern, R. S. Hill, G. Hinshaw, A. Kogut, E. Komatsu, D. Larson, M. Limon, S. S. Meyer, M. R. Nolta, N. Odegard, L. Page, K. M. Smith, D. N. Spergel, G. S. Tucker, J. L. Weiland, E. Wollack, and E. L. Wright. Seven-year Wilkinson Microwave Anisotropy Probe (WMAP) Observations: Sky Maps, Systematic Errors, and Basic Results. , 192:14, February 2011.

[4] Nikhil Padmanabhan and Douglas P. Finkbeiner. Detecting dark matter annihilation with cmb polarization: Signatures and experimental prospects. *Phys. Rev. D*, 72:023508, Jul 2005.

[5] Matias Zaldarriaga, David N. Spergel, and Uro Seljak. Microwave background constraints on cosmological parameters. *The Astrophysical Journal*, 488(1):1, 1997.